

Discoveries of waves in dusty plasmas

A. A. MAMUN† and P. K. SHUKLA

RUB International Chair, International Centre for Advanced Studies in Physical Sciences,
Faculty of Physics and Astronomy, Ruhr-Universität Bochum, D-44780 Bochum, Germany
(profshukla@yahoo.de, ps@tp4.rub.de)

(Received 12 August 2010 and accepted 2 September 2010)

Abstract. The basic features of dusty plasmas, particularly basic characteristics of dust in a plasma, and typical dusty plasma parameters for different space and laboratory plasma conditions, are presented. The complexity and the diversity of the field of dusty plasma physics are briefly discussed. Theoretical and experimental discoveries of linear and nonlinear features of waves, particularly dust-ion-acoustic and dust-acoustic waves, in dusty plasmas are reviewed.

1. Introduction

A plasma with dust is roughly known as a dusty plasma [1–9]. Dust particles in a plasma are not neutral, but are charged either negatively or positively depending on the ambient plasma environments. The mass (million to billion times heavier than ions), size (nm to mm) and charge (few hundred to hundred thousand electron or proton charges) of dust are not, in general, constant, but vary with space and time. The addition of such dust (of variable mass, size and charge), therefore, makes a plasma system very complex. A plasma with dust is, therefore, known as a complex plasma. At equilibrium (in absence of any external disturbance) like an electron–ion plasma, a dusty plasma is also macroscopically neutral. This means that in an equilibrium (with no external force present), the net resulting electric charge in a dusty plasma is zero. Therefore, the equilibrium charge neutrality condition in a dusty plasma reads $q_i n_{i0} = en_{e0} - q_{d0} n_{d0}$, where n_{s0} is the number density of the plasma species s (s equals e for electrons, i for ions and d for dust) at equilibrium, $q_i = Z_i e$ is the ion charge (we note that the ion charge state $Z_i = 1$ will be used in this paper), $q_{d0} = Z_d e$ ($-Z_d e$) is the equilibrium dust charge when the grains are positively (negatively) charged, e is the magnitude of the electron charge and Z_d is the number of charges residing onto the dust grain surface. Typically, a dust grain acquires one thousand to several hundred thousands of elementary charges and $Z_d n_{d0}$ could be comparable to n_{i0} , even for $n_{d0} \ll n_{i0}$. However, in many laboratory and space plasma situations, the most of the background electrons could stick onto the dust grain surface during the charging processes, and as a result one might encounter a significant depletion of the electron number density in the ambient dusty plasma. Accordingly, for negatively charged dust grains the equilibrium charge neutrality condition is then replaced by $n_{i0} \approx Z_d n_{d0}$. It should be noted here that a complete depletion of the electrons is not possible, because the minimum value of the ratio

† Permanent address: Department of physics, Jahangirnagar University, Savar, Dhaka 1342, Bangladesh.

of electron number density to ion number density turns out to be the square root of the ratio of electron mass to ion mass when electron and ion temperatures are approximately equal, and the grain surface potential approaches to zero.

The presence of charged dust particles significantly modifies the plasma Debye-radius. The dusty plasma Debye-radius λ_D is defined as [5] $1/\lambda_D^2 = 1/\lambda_{De}^2 + 1/\lambda_{Di}^2$, where $\lambda_{De,i} = (k_B T_{e,i}/4\pi n_{e0,i} e^2)^{1/2}$ (with T_e (T_i) being the electron (ion) temperature, and k_B being the Boltzmann constant). The quantity λ_D is a measure of the shielding distance or the thickness of the sheath. For a dusty plasma with negatively charged dust grains, we have $n_{e0} \ll n_{i0}$ and $T_e \geq T_i$, i.e. $\lambda_{De} \gg \lambda_{Di}$. Accordingly, we have $\lambda_D \simeq \lambda_{Di}$. This means that the shielding distance or the thickness of the sheath in a dusty plasma with negatively charged dust is mainly determined by the temperature and number density of the ions. However, when the dust particles are positively charged, and most of the ions are attached onto the dust grain surface, i.e. when $T_e n_{i0} \ll T_i n_{e0}$, we have $\lambda_{De} \ll \lambda_{Di}$. The latter corresponds to $\lambda_D \simeq \lambda_{De}$. This means that in a dusty plasma with positively charged dust, the shielding distance or the thickness of the sheath is mainly determined by the temperature and density of the electrons.

Similar to the usual electron–ion plasma, an important dusty plasma property is the stability of its macroscopic space charge neutrality. When a plasma is instantaneously disturbed from its equilibrium, the resulting internal space charge field gives rise to collective particle motions, which tend to restore the original charge neutrality. These collective motions are characterized by a natural frequency of oscillations known as the plasma frequency, which is defined as $\omega_p^2 = \sum_s \omega_{ps}^2$, where $\omega_{ps} = (4\pi n_{s0} q_s^2 / m_s)^{1/2}$, with m_s being the mass of the species s . The other important characteristic frequencies are associated with the collisions of the plasma particles (electrons, ions and dust) with stationary neutral atoms or molecules. These are electron-neutral collision frequency, ν_{en} , ion-neutral collision frequency, ν_{in} and dust-neutral collision frequency, ν_{dn} , respectively. The collision frequency, ν_{sn} , for scattering of the plasma species s by stationary neutrals is $\nu_{sn} = n_n \sigma_s^n V_{Ts}$, where n_n is the neutral number density, σ_s^n is the scattering cross section (which is typically of the order of 5×10^{-15} cm², and depends weakly on the temperature, T_s), and $V_{Ts} = (k_B T_s / m_s)^{1/2}$ is the thermal speed of the species s . The collisions of the plasma particles with stationary neutrals tend to damp their collective oscillations, and gradually diminish their amplitudes. The oscillations will be slightly damped only when the collision frequency ν_{sn} is smaller than the plasma frequency ω_p , i.e. $\nu_{en}, \nu_{in}, \nu_{dn} < \omega_p$.

Dusty plasmas are rather ubiquitous in space [1–5]. There are a number of well-known systems in space, such as inter-planetary space, interstellar medium, interstellar or molecular clouds, circumstellar clouds, comets, solar system, planetary rings, noctilucent clouds (NLCs), earth’s environments, etc., where charged dust particles are always present. The interstellar space (space between the stars) is filled up with a vast medium of gas and dust. The gas content of the interstellar medium continually decreases with time as new generations of stars are formed during the collapse of giant molecular clouds. The collapse and fragmentation of these clouds give rise to the formation of stellar clusters. The presence of dust in interstellar or circumstellar clouds has been known for a long time (from star reddening and infrared emission). The dust grains in interstellar or circumstellar clouds are dielectric (ice, silicates, etc.) and metallic (graphite, magnetite, amorphous carbon, etc.). The solar system is also full of dust. The existence of dust in the early solar

Table 1. Typical dusty plasma parameters in interstellar space.

Characteristics	Interstellar clouds	Zodiacal dust disc	Haley's comet
n_e (cm ⁻³)	10 ⁻⁴ –10 ⁻³	1–10	10 ² –10 ⁴
T_e (K)	10–20	10 ⁴ –10 ⁵	10 ³ –10 ⁴
n_d (cm ⁻³)	10 ⁻⁷ –10 ⁻⁶	10 ⁻¹² –10 ⁻¹¹	10 ⁻⁸ –10 ⁻³
r_d (μm)	0.1–0.5	1–10	0.1–10

Table 2. Typical dusty plasma parameters in Saturn's E-ring, F-ring and spokes.

Characteristics	E-ring	F-ring	Spokes
n_e (cm ⁻³)	10–20	10–20	0.1–10 ²
T_e (K)	10 ⁵ –10 ⁶	10 ⁵ –10 ⁶	10 ⁴ –10 ⁵
n_d (cm ⁻³)	10 ⁻⁷ –10 ⁻⁶	1–10	0.5–1.5
r_d (μm)	0.1–0.5	1–10	0.5–1.5

Table 3. Typical dusty plasma parameters in NLCs, rocket exhausts and flames.

Characteristics	NLCs	Rocket exhausts	Flames
n_e (cm ⁻³)	10 ³ –10 ⁴	10 ¹² –10 ¹³	10 ¹¹ –10 ¹²
T_e (K)	50–10 ²	10 ³ –10 ⁴	10 ³ –10 ⁴
n_d (cm ⁻³)	10–10 ²	10 ⁷ –10 ⁸	10 ¹⁰ –10 ¹¹
r_d (μm)	0.1–1	0.1–1	0.01–0.1

nebula has long been advocated by the Nobel laureate, Hannes Alfvén [10]. The coagulation of the dust grains in the solar nebula would have led to 'planetesimals', from where comets and planets have been formed. The physical properties (such as size, mass, density, charge, etc.) of such dust grains vary depending on their origin and surroundings. The origins of the dust grains in the solar system are, for example, micro-meteoroids, space debris, man-made pollution, lunar ejecta, etc.

It is not sufficient to mention only the occurrence of dusty plasmas in space and laboratory devices, but it is very important to provide values of the dusty plasma parameters available up to now. Tables 1–4 provide us the values of these dusty plasma parameters collected from the available literature [1–25]. Tables 1–4 also show typical dusty plasma parameters for different space and laboratory plasma conditions, and will help us to understand the basic physics of dust in plasmas. The physics of mobile/immobile dust, which have variable size, charge and mass, arises unsolvable complexities and makes the field of dusty plasma physics (DPP) very rapidly growing (as indicated in Fig. 1) and infinitely large (as indicated in Fig. 2). The DPP has, therefore, become an outstanding, challenging and rapidly growing (as indicated in Fig. 1) research field not only because dust particles are ubiquitous in most space [1–9] and laboratory plasmas [11–25], and involve unsolvable complexities but also because it has introduced a new but infinitely large research domain (as indicated in Fig. 2). One of the interesting research areas of DPP is introduced by 'collective processes in dusty plasmas', which introduce a great variety of new phenomena associated with waves and instabilities [26–78]. These play a vital role in understanding different interesting phenomena in

Table 4. Typical dusty plasma parameters in laboratory devices.

Characteristics	Q-machine	DC discharges	RF discharges
n_e (cm ⁻³)	10 ⁶ –10 ⁷	10 ⁹ –10 ¹⁰	10 ⁹ –10 ¹⁰
T_e (K)	10 ³ –10 ⁴	10 ⁴ –10 ⁵	10 ⁴ –10 ⁵
n_d (cm ⁻³)	10 ³ –10 ⁴	10 ³ –10 ⁴	10 ⁵ –10 ⁶
r_d (μm)	10–20 (Al ₂ O ₃)	1–5 (Al); 60–65 (glass)	5–10 (SiO ₂)
Z_d	10 ³ –10 ⁴	10 ⁵ –10 ⁶	10 ³ –10 ⁴

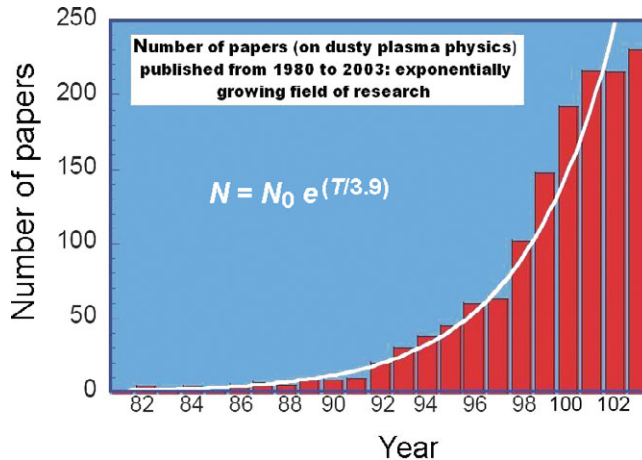


Figure 1. (Colour online) Schematic of the research field of DPP is growing exponentially since 1985 (courtesy: Prof. R. L. Merlino). This is based on ‘inspec database; subject heading: dusty plasma(s)’. The solid curve represents $N = N_0 \exp(T/3.9)$.

astrophysical and space environments, such as in inter-planetary space, interstellar medium, interstellar or molecular clouds, comets, planetary rings, noctiluscent clouds (NLCs), earth’s environments, etc. [1–9].

These collective dust-plasma interactions do not only modify the existing plasma wave spectra [26, 27] but also introduce a number of new eigenmodes, such as dust ion-acoustic (DIA) waves [30], dust-acoustic (DA) waves [28], dust-lattice (DL) waves [41, 44], dust-lower-hybrid (DLH) waves [40], dust ion-cyclotron (DIC) waves [11], dust-cyclotron (DC) waves [37], Shukla-Varma (SV) mode [33], dust shear-Alfvén (DSA) waves [36], dust-magnetoacoustic (DM) waves [35], etc. All of these waves or modes have not yet been experimentally observed. But a number of new novel eigenmodes, particularly DIA, DA and DL waves, have already been experimentally verified by different laboratory experiments [13–16]. The linear and nonlinear features of these waves have been rigorously investigated by a large number of authors during last two decades [26–78]. We, in this short review paper, have attempted to provide a brief review of theoretical and experimental discoveries of these linear and nonlinear features of some novel new eigenmodes in dusty plasmas, particularly DIA and DA waves (DAWs).

The manuscript is organized as follows. The theoretically predicted and experimentally observed linear and nonlinear features of DIA waves are reviewed in §2, and those of DAWs are reviewed in §3. A brief discussion is presented in §4.

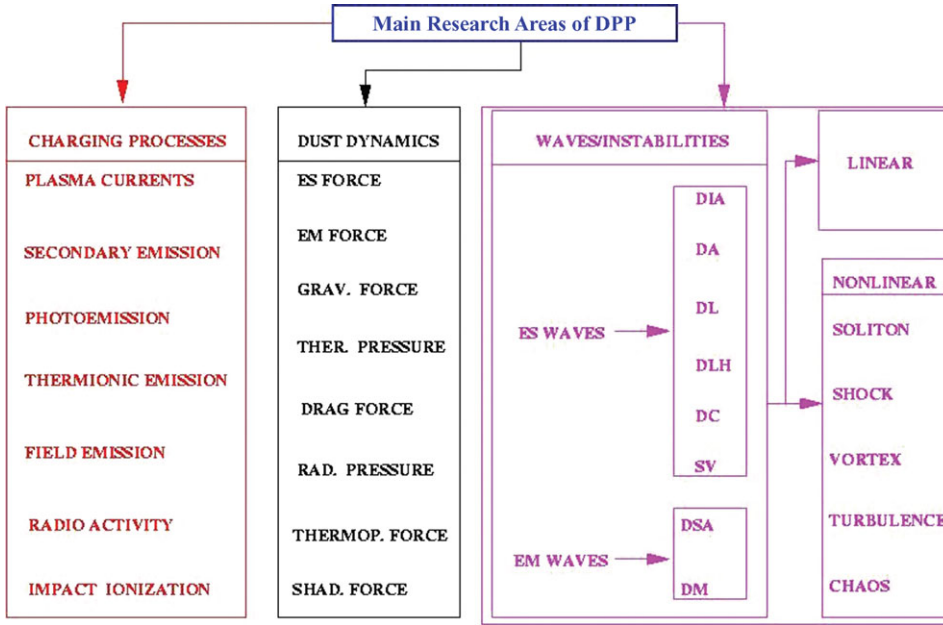


Figure 2. (Colour online) The main research areas of DPP indicating that the field of DPP is new, but infinitely large. Here GRAV. = gravitational, THER. = thermal, RAD. = radiation, THERMOP. = thermophoretic, SHAD. = shadowing and the other notations have already been defined.

2. DIA waves

Shukla and Silin [30] have first theoretically shown that due to the conservation of equilibrium charge density ($n_{e0} + Z_d n_{d0} = n_{i0}$), and the strong inequality, $n_{e0} \ll n_{i0}$, a dusty plasma (with negatively charged static dust) supports low-frequency DIA waves (DIAWs) with phase speed much smaller (larger) than electron (ion) thermal speed. The dispersion relation (a relation between the wave frequency ω and the wave number k) of the linear DIAWs [30] is

$$\frac{\omega}{k} = \left(\frac{1}{1 - \mu} \right)^{\frac{1}{2}} \frac{C_i}{\sqrt{1 + k^2 \lambda_{De}^2}}, \quad (2.1)$$

where $C_i = (k_B T_e / m_i)^{1/2}$ is the ion-acoustic speed and $\mu = Z_d n_{d0} / n_{i0}$. When we consider a long wavelength limit (viz. $k \lambda_{De} \ll 1$), the dispersion relation for the DIAWs becomes $\omega = k C_i / \sqrt{1 - \mu}$. This form of spectrum is similar to the usual ion-acoustic waves (IAWs) for a plasma with $n_{i0} = n_{e0}$ (corresponding to $\mu = 0$) and $T_i \ll T_e$. However, in a dusty plasma we usually have $n_{i0} \gg n_{e0}$ and $T_i \simeq T_e$. Therefore, a dusty plasma cannot support the usual IAWs, but can do the DIAWs of Shukla and Silin [30]. The phase speed ω/k of the DIAWs is larger than C_i because of $n_{i0} \gg n_{e0}$ for negatively charged dust grains. The increase in the phase velocity is attributed to the electron density depletion in the background plasma so that the electron Debye radius becomes larger. As a result, there appears a stronger space charge electric field, which is responsible for the enhanced phase velocity of the DIAWs. The DIAWs have been observed in laboratory experiments [14,16]. The experimental conditions for the

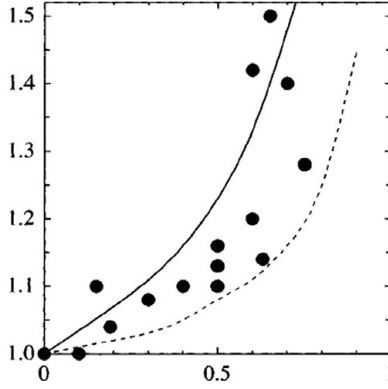


Figure 3. The normalized phase speed versus μ curves for grid-launched DIAWs (Merlino et al. [16]). Measured normalized phase speed (along vertical or y -axis) as a function of μ (along horizontal or x -axis): solid dots (laboratory measurement), solid curve (theoretical measurement without plasma drift) and dotted curve (theoretical measurement with a plasma drift of twice the acoustic speed). The phase speed is normalized by its value without dust ($\mu = 0$).

observation of DIAWs [14, 16] are $n_e \simeq n_i \simeq 10^5\text{--}10^9 \text{ cm}^{-3}$, $T_e \simeq T_i \simeq 0.2\text{--}0.3 \text{ eV}$, $r_d \simeq 1.5\text{--}7.5 \mu\text{m}$ (kaolin dust). A good agreement between theory [30] and laboratory experiments [14, 16] is shown in Fig. 3. Theoretical analysis (based on both fluid and kinetic models) and laboratory experiments confirmed that the presence of charged dust causes to increase the phase speed, but causes to decrease the Landau damping. The difference between the IAWs and DIAWs is that the IAWs are subject to ion Landau damping, which is severe for $T_e \simeq T_i$, but this is not the case for DIAWs, where wave-particle resonance (at phase speed equal to ion thermal speed) no longer holds.

There are many space and laboratory dusty plasma situations, where the amplitude of DIAWs is very large, and the linear theory is no longer valid. The large amplitude DIAWs are found to propagate as either solitary or shock waves (SWs). We now (in next two subsections) briefly explain theoretical and experimental observations of solitary and shock structures associated with these DIAWs.

2.1. DIA solitary waves

We consider an unmagnetized dusty plasma whose constituents are inertial ions, Boltzmann electrons and negatively charged immobile dust particles. The nonlinear dynamics of the DIAWs, whose phase speed is much smaller (larger) than the electron (ion) thermal speed, is governed by

$$\frac{\partial n_i}{\partial t} + \frac{\partial}{\partial x}(n_i u_i) = 0, \quad (2.2)$$

$$\frac{\partial u_i}{\partial t} + u_i \frac{\partial u_i}{\partial x} = -\frac{\partial \phi}{\partial x}, \quad (2.3)$$

$$\frac{\partial^2 \phi}{\partial x^2} = (1 - \mu) \exp(\phi) - n_i + \mu, \quad (2.4)$$

where n_i is the ion number density normalized by its equilibrium value n_{i0} , u_i is the ion fluid speed normalized by C_i , and ϕ is the electrostatic wave potential normalized by $k_B T_e/e$. The time and space variables are in units of the ion plasma period ω_{pi}^{-1} and the Debye radius $\lambda_{Dm} = (k_B T_e/4\pi n_{i0} e^2)^{1/2}$, respectively.

To study the small but finite amplitude DIA SWs, we use the reductive perturbation method [87], i.e. we first introduce the stretched coordinates:

$$\left. \begin{aligned} \zeta &= \epsilon^{1/2}(x - V_p t), \\ \tau &= \epsilon^{3/2}t, \end{aligned} \right\} \quad (2.5)$$

where ϵ is an expansion parameter ($0 < \epsilon < 1$) and $V_p = \omega/kC_i$, and then expand n_i , u_i and ϕ in power series of ϵ :

$$\left. \begin{aligned} n_i &= 1 + \epsilon n_i^{(1)} + \epsilon^2 n_i^{(2)} + \dots, \\ u_i &= 0 + \epsilon u_i^{(1)} + \epsilon^2 u_i^{(2)} + \dots, \\ \phi &= 0 + \epsilon \phi^{(1)} + \epsilon^2 \phi^{(2)} + \dots \end{aligned} \right\} \quad (2.6)$$

We then develop equations in various powers of ϵ . To the lowest order in ϵ , (2.2)–(2.4) give $n_i^{(1)} = u_i^{(1)}/V_p$, $u_i^{(1)} = \phi^{(1)}/V_p$ and $V_p = 1/\sqrt{1-\mu}$. To the next higher order in ϵ , we obtain a set of equations (for $n_i^{(2)}$, $u_i^{(2)}$ and $\phi^{(2)}$), which reduces to a Korteweg-de Vries (K-dV) equation,

$$\frac{\partial \phi^{(1)}}{\partial \tau} + A \phi^{(1)} \frac{\partial \phi^{(1)}}{\partial \zeta} + B \frac{\partial^3 \phi^{(1)}}{\partial \zeta^3} = 0, \quad (2.7)$$

where

$$A = \frac{3}{2\sqrt{1-\mu}} \left(\frac{2}{3} - \mu \right), \quad (2.8)$$

$$B = \frac{1}{2(1-\mu)^{3/2}}. \quad (2.9)$$

Now, for a frame moving with a speed U_0 , the stationary SW solution of (2.7) is

$$\phi^{(1)} = \left(\frac{3U_0}{A} \right) \operatorname{sech}^2 \left[\sqrt{\frac{U_0}{4B}} (\zeta - U_0 \tau) \right]. \quad (2.10)$$

It is obvious from (2.8) and (2.10) that for $\mu < (>)2/3$, a dusty plasma supports compressive (rarefactive) DIA SWs, which are associated with a positive (negative) potential, and that the amplitude and the width of these SWs depend on U_0 and μ . It is also obvious that as U_0 increases, the amplitude ($3U_0/A$) increases, but the width ($\sqrt{4B/U_0}$) decreases. The variation of amplitude and width with μ has been graphically shown by many authors during last few years (e.g. Mamun and Shukla [55]).

To study the arbitrary amplitude DIA SWs [32] by the pseudo-potential approach, we make all the dependent variables depend only on a single variable $\xi = x - Mt$, where M is the DIA SW speed normalized by C_i , use the steady state condition, impose the appropriate boundary conditions for localized solitary structures, namely $n_i \rightarrow i$, $u_i \rightarrow 0$, $\phi \rightarrow 0$ and $d\phi/d\xi \rightarrow 0$ at $\xi \rightarrow \pm\infty$ and finally reduce (2.2)–(2.4) to a

single equation of the form [88,89]

$$\frac{1}{2} \left(\frac{d\phi}{d\xi} \right)^2 + V(\phi) = 0, \quad (2.11)$$

where

$$V(\phi) = 1 - \mu + M^2 - \mu\phi - (1 - \mu)\exp(\phi) - M^2 \sqrt{1 - \frac{2\phi}{M^2}}. \quad (2.12)$$

The integration constant is chosen in such a way that $V(\phi) = 0$ at $\phi = 0$. Equation (2.11) represents an ‘energy integral’ for an oscillating particle of unit mass, with pseudo-position ϕ , pseudo-time ξ and pseudo-potential $V(\phi)$. We note that M is not the exact Mach number, because it is normalized by C_i , which is not the exact phase speed of linear DIAWs.

We can find that $V(\phi) = dV(\phi)/d\xi = 0$ at $\phi = 0$. Therefore, SW solutions of (2.11) exist if (i) $(d^2V/d\phi^2)_{\phi=0} \leq 0$, so that the fixed point at the origin is unstable (‘equal’ sign corresponds to an unstable point, at least, on one side), and (ii) $V(\phi) < 0$, when $0 > \phi > \phi_{\max}$ for the compressive DIA SWs and $\phi_{\min} < \phi < 0$ for the rarefactive DIA SWs, where ϕ_{\max} (ϕ_{\min}) is the maximum (minimum) value of ϕ for which $V(\phi_{\max}) = V(\phi_{\min}) = 0$. The condition (i) is satisfied when

$$M \geq M_c = V_p = \frac{1}{\sqrt{1 - \mu}}. \quad (2.13)$$

To examine whether the condition (ii) is satisfied or not, one has to directly examine the pseudo-potential $V(\phi)$, at least, for the study of the arbitrary amplitude DIA SWs. Bharuthram and Shukla [32] have investigated the properties of the arbitrary amplitude DIA SWs by analyzing the pseudo-potential $V(\phi)$. They have found that for $\mu < 2/3$ only compressive DIA SWs exist, but for $\mu > 2/3$, compressive DIA SWs coexist with rarefactive ones. The small as well as large (arbitrary) amplitude DIA SWs have been rigorously investigated by many others for different dusty plasma situations, e.g. non-planar geometry [55], adiabaticity of electrons and ions [68], non-thermal electron distribution [74], electronegative dusty plasma [75] etc. The basic features of the DIA SWs are experimentally identified by Nakamura and Sharma [22]. The experimentally observed basic features (speed, amplitude and width) of the DIA SWs are shown in Fig. 4. We note that no rarefactive DIA SW is observed under laboratory conditions of Nakamura and Sharma [22], where μ is less than its critical value (2/3) for the existence of rarefactive SWs (rarefaction of ion number density).

2.2. DIA shock waves

To study DIA shock waves, we consider a dissipative dusty plasma system where dissipation may arise from either kinematic viscosity [19,46] or dust charge fluctuation [53,57]. The nonlinear dynamics of the DIAWs, whose phase speed is much smaller (larger) than the electron (ion) thermal speed, in such a dissipative dusty plasma system is, therefore, described by (2.2), (2.4) and

$$\frac{\partial u_i}{\partial t} + u_i \frac{\partial u_i}{\partial x} = -\frac{\partial \phi}{\partial x} - \eta_i \frac{\partial^2 u_i}{\partial x^2}, \quad (2.14)$$

where $\eta_i = \mu_i / \omega_{pi} \lambda_{Dm}^2$ with μ_i being the kinematic viscosity.

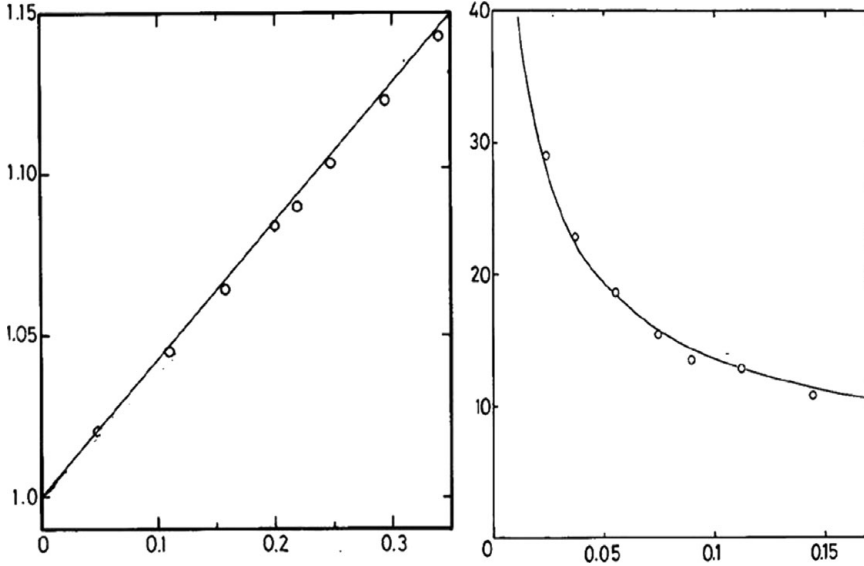


Figure 4. Mach number (vertical-axis of right figure) and normalized (normalized by λ_{De}) width (vertical-axis of left figure) versus normalized height (ion number density compression normalized by electron equilibrium number density) of the DIA SWs (Nakamura and Sharma [22]): solid curve (theoretical) and solid circles (experimental) for $n_{i0}/n_{e0} = 1.6$, i.e. $\mu = 0.375$.

Now, using the same stretched co-ordinates (defined by (2.5)) and expansion series (defined by (2.6)), and following the same technique as we have used in the previous section, one can readily obtain the following K-dV-Burgers equation:

$$\frac{\partial \phi^{(1)}}{\partial \tau} + A \phi^{(1)} \frac{\partial \phi^{(1)}}{\partial \zeta} + B \frac{\partial^3 \phi^{(1)}}{\partial \zeta^3} = C \frac{\partial^2 \phi^{(1)}}{\partial \zeta^2}, \quad (2.15)$$

where A , B and C are, respectively, given by (2.8), (2.9) and $C = \eta_{i0}/2$, in which η_{i0} is defined by $\eta_i = \epsilon^{1/2} \eta_{i0}$. An exact analytical solution of (2.15) is not possible. However, we can deduce some approximate analytical solutions of (2.15) by using the transformation $\xi = \zeta - U_0 \tau$, the steady-state condition and the appropriate boundary conditions, viz. $\phi \rightarrow 0$, $d\phi/d\xi \rightarrow 0$, $d^2\phi/d\xi^2 \rightarrow 0$ at $\xi \rightarrow \infty$. The latter allow us to express (2.15) as

$$B \frac{d^2 \phi}{d\xi^2} - C \frac{d\phi}{d\xi} + \frac{A}{2} \phi^2 - U_0 \phi = 0, \quad (2.16)$$

where $\phi = \phi^{(1)}$ is used just to avoid writing superscripts again and again. To analyze (2.16), we can use a simple mechanical analogy [90] based on a fact that it has a form of an equation of motion for a pseudo particle of mass B , of pseudo time ξ and pseudo position ϕ in a force field with potential

$$V(\phi) = \frac{A}{6} \phi^3 - \frac{U_0}{2} \phi^2, \quad (2.17)$$

and a frictional force with the coefficient C . If the frictional force is absent, the quasi-particle entering from the left will go to the right-hand side of the well ($\phi < 0$), reflect and return to $\phi = 0$, thus making a single transit. This corresponds to the

DIA SWs defined by (2.10). However, as in (2.16), a frictional force is practically present, i.e. the particle suffers a loss of energy, it will never return $\phi=0$, but will oscillate about some negative value of ϕ corresponding to the minimum of $V(\phi)$. We assume that at pseudo time $\xi = \infty$, the quasi-particle is located at the coordinate origin, i.e. $\phi(\infty)=0$, and at pseudo time $\xi = -\infty$, the quasi-particle is located at a point corresponding to the minimum of $V(\phi)$, i.e. $\phi(-\infty)=2U_0/A$. Thus, the solution of (2.16) describes a shock wave whose speed U_0 is related to the extreme values $\phi(\infty)=0$ and $\phi(-\infty)=2U_0/A$ by $\phi(-\infty) - \phi(\infty) = 2U_0/A$.

The nature of these shock structures depends on the relative values between the dispersive and dissipative coefficients B and C . If the value of C is very small, the energy of the particle decreases very slowly, and the first few oscillations at the wave front will be close to SWs defined by (2.10). However, if the value of C is larger than a certain critical value, the motion of the particle will be aperiodic, and we obtain a shock wave with a monotonic structure.

We now determine the condition for monotonic and oscillatory shock profiles by investigating the asymptotic behavior of the solutions of (2.16) for $\xi \rightarrow -\infty$. We first substitute $\phi(\xi) = \phi_0 + \Phi(\xi)$, where $\Phi \ll \phi_0$, into (2.16), and then linearize it with respect to Φ in order to obtain

$$B \frac{d^2 \Phi}{d\xi^2} - C \frac{\partial \Phi}{\partial \xi} + U_0 \Phi = 0. \quad (2.18)$$

The solutions of (2.18) are proportional to $\exp(p\xi)$, where p is given by

$$p = \frac{C \pm \sqrt{C^2 - 4BU_0}}{2B}. \quad (2.19)$$

It turns out that the shock wave has a monotonic profile for $S_c = C/2\sqrt{BU_0} > 1$ and an oscillatory profile for $S_c < 1$.

The limit $S_c \gg 1$ gives rise to a simple Burgers equation ((2.15) with $B=0$), which can be directly obtained by using different stretched co-ordinates [71–73]

$$\left. \begin{aligned} \zeta &= \epsilon(x - V_p t), \\ \tau &= \epsilon^2 t. \end{aligned} \right\} \quad (2.20)$$

The advantage of this new stretched co-ordinates is that it does not require the additional assumption $\eta_i = \epsilon^{1/2} \eta_{i0}$, and so C becomes $C = \eta_i/2$. The solution of this Burgers equation ((2.15) with $B=0$) is given by

$$\phi^{(1)} \simeq \frac{U_0}{A} \left[1 - \tanh \left\{ (\zeta - U_0 \tau) \frac{U_0}{2C} \right\} \right]. \quad (2.21)$$

It is obvious from (2.8) and (2.21) that for $\mu < (>)2/3$, a dusty plasma supports compressive (rarefactive) DIA shock structures, which are associated with a positive (negative) potential, and that the amplitude of these shock structures depends on U_0 and μ , whereas their width depends on U_0 and η_i . It is also obvious that as U_0 increases, the amplitude ($3U_0/A$) increases, but the width ($2C/U_0$) decreases. The variation of amplitude with μ is the same as that for the DIA SWs. However, the shock width is directly proportional to η_i . The properties of DIA shock structures, which are formed due to either kinematic viscosity [19,46] or dust charge fluctuation [53,57], have been rigorously investigated by many others for different dusty plasma situations [46, 53, 57, 61, 73, 76].

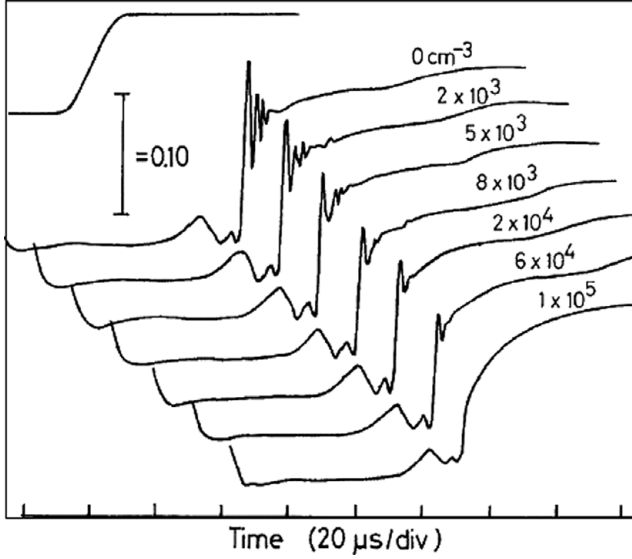


Figure 5. The variation of the plasma number density with time at a fixed probe position (12 cm) showing the transition of an oscillatory shock to a monotonic shock when the dust particle number density is increased (Nakamura et al. [19]).

The basic features of DIA SWs are experimentally identified by Nakamura et al. [19]. The experimentally observed DIA shock structures [19] are shown in Fig. 5. It reveals that the oscillatory wave structure behind the shock becomes less in number with increasing the dust particle number density, and finally completely disappears at a sufficiently high dust particle number density leaving only the laminar shock front. The shock speed also increases with increasing the dust particle number density. It is also noted that the particle density behind the shock remains constant, although the amplitude of the shock front (steepened part) seems to decrease when the dust particle number density is increased. The effect of the dust particle number density on the ion-acoustic compressional pulses has also been experimentally studied by Luo et al. [20], who observed a steepening of the ion-acoustic pulses as they propagated through a dusty plasma if the percentage of the negative charge in the plasma on the dust grains was about 75% or more.

3. DA waves

Rao et al. [28] theoretically predicted the existence of extremely low-phase velocity (in comparison with the electron and ion thermal speeds) DAWs in an unmagnetized dusty plasma whose constituents are an inertial charged dust fluid and Boltzmann ions and electrons. Thus, in the DAWs the inertia is provided by the dust particle mass and the restoring force comes from the pressures of ions and electrons. The dispersion relation for the DAWs, whose phase speed (ω/k) is much smaller (larger) than the ion (dust) thermal speed, is given by [28]

$$\frac{\omega}{k} = \frac{C_d}{\sqrt{1 + k^2 \lambda_D^2}}, \quad (3.1)$$

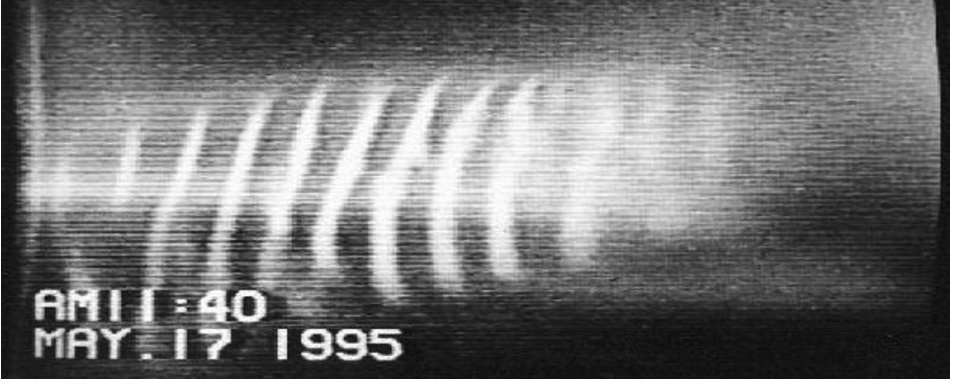


Figure 6. A typical single-frame image of a dust-acoustic wave pattern recorded in the video camera (Barkan et al. [13]).

where $\lambda_D = (\lambda_{De}^{-2} + \lambda_{Di}^{-2})^{-1/2}$ is the global screening length, and $C_d = \omega_{pd} \lambda_D$ is the dust-acoustic speed. It is obvious that one cannot obtain the DAWs without the consideration of dust dynamics. The theoretical prediction of Rao et al. [28] has been conclusively verified by a number of laboratory experiments [13, 18]. The experimental conditions for observation of DAWs [13, 18] are $n_e \simeq n_i \simeq 10^8 - 10^9 \text{ cm}^{-3}$, $T_e \simeq 2 - 3 \text{ eV}$, $T_i \simeq 0.025 \text{ eV}$, $r_d \simeq 1 - 7 \text{ } \mu\text{m}$ (kaolin dust), $Z_d \sim 10^3$ and $n_d \simeq 10^5 \text{ cm}^{-3}$. The image of these experimentally observed DAWs is shown in Fig. 6. Theoretical analysis [28] and laboratory experiments [13, 18] confirmed that the DAWs, which are observed even with naked eyes, are very low-frequency ($\sim 15 \text{ Hz}$) waves, whose speed and wavelength are $\sim 9 \text{ cm s}^{-1}$ and $\sim 0.6 \text{ cm}$, respectively.

3.1. DA solitary waves

We consider a three-component dusty plasma system consisting of negatively charged dust and Boltzmann-distributed ions and electrons. The nonlinear dynamics of the low-phase speed (lying between the ion and dust thermal speeds) DAWs is governed by [28]

$$\frac{\partial n_d}{\partial t} + \frac{\partial}{\partial x}(n_d u_d) = 0, \quad (3.2)$$

$$\frac{\partial u_d}{\partial t} + u_d \frac{\partial u_d}{\partial x} = \frac{\partial \phi}{\partial x}, \quad (3.3)$$

$$\frac{\partial^2 \phi}{\partial x^2} = n_d - \left(\frac{1}{1 - \beta} \right) e^{-\phi} + \left(\frac{\beta}{1 - \beta} \right) e^{\alpha \phi}, \quad (3.4)$$

where n_d is the dust number density normalized by n_{d0} , u_d is the dust fluid speed normalized by $c_d = (Z_d k_B T_i / m_d)^{1/2}$, ϕ is the electrostatic wave potential normalized by $k_B T_i / e$, $\beta = n_{e0} / n_{i0}$ and $\alpha = T_i / T_e$. The time and space variables are in the units of the dust plasma period ω_{pd}^{-1} and the Debye length $\lambda_{Dd} = (k_B T_i / 4\pi Z_d n_{d0} e^2)^{1/2}$, respectively.

To study small but finite amplitude DA SWs, we use the reductive perturbation method [87], i.e. we first employ the stretched coordinates:

$$\left. \begin{aligned} \zeta &= \epsilon^{1/2}(x - v_p t), \\ \tau &= \epsilon^{3/2}t, \end{aligned} \right\} \quad (3.5)$$

where $v_p = \omega/kc_d$, and expand n_d , u_d and φ in power series of ϵ :

$$\left. \begin{aligned} n_d &= 1 + \epsilon n_d^{(1)} + \epsilon^2 n_d^{(2)} + \dots, \\ u_d &= 0 + \epsilon u_d^{(1)} + \epsilon^2 u_d^{(2)} + \dots, \\ \varphi &= 0 + \epsilon \varphi^{(1)} + \epsilon^2 \varphi^{(2)} + \dots, \end{aligned} \right\} \quad (3.6)$$

and finally develop equations in various powers of ϵ . To the lowest order in ϵ , (3.2)–(3.4) give $n_d^{(1)} = u_d^{(1)}/v_p$, $u_d^{(1)} = -\varphi^{(1)}/v_p$ and $v_p = [(1 - \beta)/(1 + \alpha\beta)]^{1/2}$. To the next higher order in ϵ , we obtain a set of equations which deduces to a K-dV equation

$$\frac{\partial \varphi^{(1)}}{\partial \tau} + A_d \varphi^{(1)} \frac{\partial \varphi^{(1)}}{\partial \zeta} + B_d \frac{\partial^3 \varphi^{(1)}}{\partial \zeta^3} = 0, \quad (3.7)$$

where

$$A_d = -\frac{v_p^3}{(1 - \beta)^2} \left[1 + (3 + \alpha\beta)\alpha\beta + \frac{1}{2}\beta(1 + \alpha^2) \right], \quad (3.8)$$

$$B_d = \frac{v_p^3}{2}. \quad (3.9)$$

Now, for a frame moving with a speed u_0 , the stationary SW solution of (3.7) is

$$\varphi^{(1)} = \left(\frac{3u_0}{A_d} \right) \operatorname{sech}^2 \left[\sqrt{\frac{u_0}{4B_d}} (\zeta - u_0\tau) \right]. \quad (3.10)$$

It is obvious from (3.8) and (3.10) that A_d is always negative for all possible values of α and β , and that the plasma system, under consideration, supports only SWs with $\varphi < 0$, but does not support any SW with $\varphi > 0$. It is also obvious that the amplitude and width of these SWs depend on u_0 , α and β . It is also obvious that as u_0 increases, the amplitude ($3u_0/A_d$) increases, but the width ($\sqrt{4B_d/u_0}$) decreases. The variation of the amplitude and width with α and β have been graphically shown by Mamun [43].

To study the arbitrary amplitude DA SWs [38, 39, 43] by the pseudo-potential approach [88, 89], we make all the dependent variables depend only on a single variable $\xi = x - \mathcal{M}t$, where \mathcal{M} is the DA SW speed normalized by c_d , use the steady state condition, impose the appropriate boundary conditions for localized solitary structures, namely $n_d \rightarrow i$, $u_d \rightarrow 0$, $\phi \rightarrow 0$ and $d\varphi/d\xi \rightarrow 0$ at $\xi \rightarrow \pm\infty$, and reduce (3.2)–(3.4) to an energy integral [88, 89]

$$\frac{1}{2} \left(\frac{d\varphi}{d\xi} \right)^2 + V(\varphi) = 0, \quad (3.11)$$

where

$$V(\varphi) = \mathcal{M}^2 + \frac{1}{1-\beta} + \frac{\beta}{\alpha(1-\beta)} - \mathcal{M}^2 \sqrt{1 + \frac{2\varphi}{\mathcal{M}^2}} - \left(\frac{1}{1-\beta} \right) \exp(-\varphi) - \left[\frac{\beta}{\alpha(1-\beta)} \right] \exp(\alpha\varphi). \quad (3.12)$$

The integration constant is chosen in such a way that $V(\varphi) = 0$ at $\varphi = 0$. We note that \mathcal{M} is not the exact Mach number, because it is normalized by c_d , which is not the exact phase speed of the linear DAWs. We can find that $V(\varphi) = dV(\varphi)/d\xi = 0$ at $\varphi = 0$. Therefore, SW solutions of (3.11) exist if (i) $(d^2V/d\varphi^2)_{\varphi=0} \leq 0$, so that the fixed point at the origin is unstable, and (ii) $V(\varphi) < 0$, when $0 > \varphi > \varphi_{\max}$ for the compressive DA SWs and when $\phi_{\min} < \phi < 0$ for the rarefactive DA SWs, where φ_{\max} (φ_{\min}) is the maximum (minimum) value of φ , for which $V(\varphi_{\max}) = V(\varphi_{\min}) = 0$. The condition (i) is satisfied when

$$\mathcal{M} \geq \mathcal{M}_c = v_p = \sqrt{\frac{1-\beta}{1+\alpha\beta}}. \quad (3.13)$$

To examine whether the condition (ii) is satisfied or not, one has to directly examine the pseudo-potential $V(\varphi)$ at least for the study of the arbitrary amplitude DA SWs. Mamun et al. [38] and Mamun [43] have investigated the properties of the arbitrary amplitude DA SWs by analyzing the pseudo-potential $V(\varphi)$. They have found that the dusty plasma, containing negatively charged dust, Boltzmann-distributed electrons and ions, supports only DA SWs with negative potential, corresponding to a hump in the dust density. The small as well as large (arbitrary) amplitude DA SWs have been rigorously investigated for different dusty plasma situations [39, 50, 56, 61, 69].

The DA SWs are experimentally observed by Bandyopadhyay et al. [24]. The experimentally observed DA SWs are shown in Fig. 7. Theoretical analysis [28, 43] and laboratory experiment [24] on DA SWs confirmed that DA SWs with a negative potential, corresponding to a hump in the dust number density, are formed. The amplitude of experimentally observed DA SWs is quite large, and hence to explain the experimental observation of Bandyopadhyay et al. [24] the theory of DA SWs [38, 43] by pseudo-potential approach is more suitable than that by reductive perturbation method [28].

3.2. DA shock waves

To study DA shock waves, we consider a dissipative (strongly coupled) dusty plasma system where dissipation arises from strong correlation among highly charged dust particles [49]. The nonlinear dynamics of the DAWs, whose phase speed is much less (greater) than ion (dust) thermal speed, in such a dissipative strongly coupled dusty plasma is governed by the well-known generalized hydrodynamic (GH) equations [91, 92], i.e. (3.2), (3.4), and

$$(1 + \tau_m D_t) \left[n_d \left(D_t u_d - \frac{\partial \varphi}{\partial x} \right) \right] = \eta_l \frac{\partial^2 u_d}{\partial x^2}, \quad (3.14)$$

where $D_\tau = 1 + \tau_m \partial/\partial t$, $D_t = \partial/\partial t + u_d \partial/\partial x$, τ_m is the viscoelastic relaxation time normalized by the dust plasma period ω_{pd}^{-1} and $\eta_l = (\tau_d/m_d n_{d0} \lambda_{Dm}^2) [\eta_b + (4/3)\zeta_b]$ is

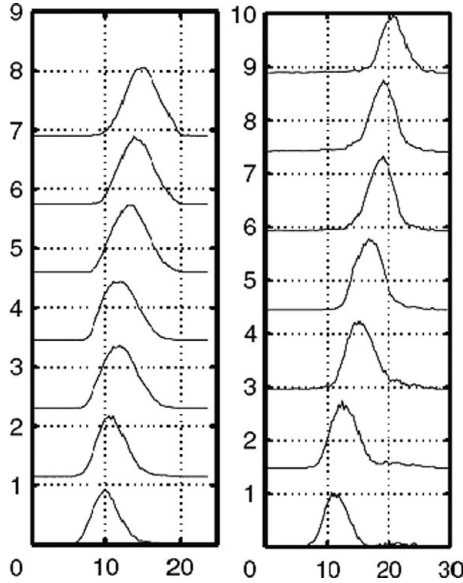


Figure 7. Experimentally observed DA SWs at two different excited pulse voltage of 60 V (left) and 120 V (right): distance (in mm) along the horizontal or x -axis and normalized dust number (n_d/n_{d0}) along vertical or y -axis (Bandyopadhyay et al. [24]).

the normalized longitudinal viscosity coefficient (with η_b and ζ_b being the bulk and shear viscosity coefficients, respectively). The description (along with the estimated values) of these transport coefficients (τ_m , η_l , η_b and ζ_b) are available in the existing literature [49, 71–73, 91–94].

Now, using the stretched co-ordinates [71–73],

$$\left. \begin{aligned} \zeta &= \epsilon(x - v_p t), \\ \tau &= \epsilon^2 t, \end{aligned} \right\} \quad (3.15)$$

and expanding n_d , u_d and ϕ in a power series of ϵ as before, and following the same technique as we have used in the previous section, one can readily obtain the Burgers equation:

$$\frac{\partial \phi^{(1)}}{\partial \tau} + A_d \phi^{(1)} \frac{\partial \phi^{(1)}}{\partial \zeta} = C_\eta \frac{\partial^2 \phi^{(1)}}{\partial \zeta^2}, \quad (3.16)$$

where A_d is given by (3.8), and C_η is given by $C_\eta = \eta_l/2$. Again, for a frame moving with a speed u_0 , the stationary shock solution of (3.16) is given by

$$\phi^{(1)} \simeq \frac{u_0}{A_d} \left[1 - \tanh \left[(\zeta - u_0 \tau) \frac{u_0}{2C_\eta} \right] \right]. \quad (3.17)$$

It is obvious from (3.8) and (3.17) that the dusty plasma under consideration supports the DA shock structures with a negative potential and that the amplitude of these shock structures depends on u_0 , α and β , whereas their width depends on u_0 and η_l . It is also obvious that as u_0 increases, the amplitude ($2u_0/A_d$) increases, but the width ($2C_\eta/u_0$) decreases. The variation of amplitude with α and β is the same as that for DA SWs. The width is directly proportional to η_l . The DA shock waves

Table 5. Discoveries of some important waves in dusty plasmas.

Waves	Theory		Experiment	
	In	By	In	By
DA	1990	Rao et al. [28]	1995	Barkan et al. [13]
DIA	1992	Shukla and Silin [29]	1996	Barkan et al. [14]
DL	1996	Melandsø [41]	1997	Homann et al. [15]
DIA shock	1999	Nakamura et al. [19]	1999	Nakamura et al. [19] Luo et al. [20]
DIA SW	1992	Bharuthram and Shukla [32]	2001	Nakamura and Sharma [22]
DA SW	1990	Rao et al. [28]	2007	Bandyopadhyay et al. [24]
	1996	Mamun et al. [38]		
	1996	Mamun [43]		
DA Shock	2001	Shukla and Mamun [49]	2009	Heinrich et al. [25]
	2004	Eliasson and Shukla [63]		
	2009	Mamun and Cairns [71]		
DIC	1990	D'Angelo [11]	1995	Barkan et al. [12]

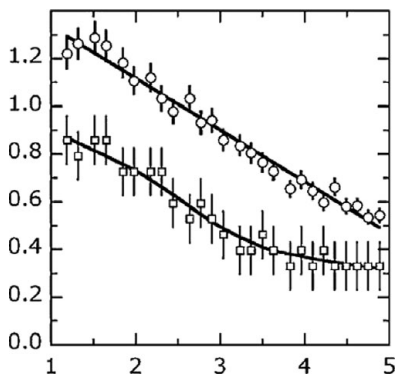


Figure 8. Shock-amplitude ($\delta I/I_{av}$) and shock-thickness (in mm) of experimentally observed DA shock-like structures (Heinrich et al. [25]): distance (in mm) along the horizontal-axis and shock-amplitude (circles or upper curve) and shock-thickness (squares or lower curve) along the vertical-axis.

have been rigorously investigated by others for different dusty plasma situations [53, 56, 61, 64, 71–73]. We note that the non-stationary DA shock-like structures predicted by Eliasson and Shukla [63] are associated with the self-steepening of the negative potential in a weakly coupled dusty plasma. This self-steepening of the negative potential, i.e. the formation of non-stationary DA shock-like structures (after a certain time) is due to the nonlinear effects.

Recently, the DA shock-like structures are observed by Heinrich et al. [25]. The basic features (amplitude and width) of these experimentally observed DA shock-like structures are shown in Fig. 8.

4. Discussion

Our universe is full of dust, i.e. dust is almost everywhere, there is no branch of space science where the physics of dust is not directly or indirectly involved. So we

Table 6. Discoveries of dust crystals, Mach cones and dust voids.

Structures	Theory		Experiment	
	In	By	In	By
Dust crystals	1986	Ikezi [79]	1995	Thomas et. al. [80] Chu et. al. [81] Hyashi et. al. [82]
Mach cones	1996	Havnes et al. [85]	1999	Samsonov et al. [84]
Dust voids	1999	Goree et al. [83]	2001	Thomas et al. [86]

cannot explain the physics of our universe without the role of dust. The physics of mobile/immobile dust, which have variable size, charge and mass, arises unsolvable complexities and makes the field of DPP very interesting (rapidly growing), and infinitely large.

The presence of dust does not only modify the existing plasma wave spectra, but also introduce new waves, e.g. DIA, DA, DL etc, which are experimentally observed. The physics of these waves must play an important significant role in understanding the properties of localized electrostatic structures in space/laboratory dusty plasmas. Theoretical and experimental discoveries of some important waves in dusty plasmas are summarized in Table 5. The discoveries in dusty plasmas are not limited to waves only. There are many other remarkable experimental discoveries, particularly discoveries of dust crystals, Mach cones, dust voids etc. in strongly coupled dusty plasmas. These are given in Table 6.

To conclude, for its infinitely large domain, versatile applications and unsolvable complexities, the field of DPP has become a challenging research topic not only for near future but also for a long period of time to come.

Acknowledgements

A. A. Mamun is grateful to the Alexander von Humboldt Stiftung (Bonn, Germany) for their financial support through the Friedrich Wilhelm Bessel Research Award, and the Jahangirnagar University for the study leave during the course of this work.

References

- [1] Goertz, C. K. 1989 *Rev. Geophys.* **27**, 271.
- [2] Mendis, D. A., Rosenberg, M. 1994 *Annu. Rev. Astron. Astrophys.* **32**, 419.
- [3] Bliokh, P., Sinitin, V. and Yaroshenko, V. 1995 *Dusty and Self-Gravitational Plasmas in Space*. Dordrecht, Netherlands: Kluwer.
- [4] Verheest, F. 2002 *Waves in Dusty Space Plasmas*. Dordrecht, Netherlands: Kluwer.
- [5] Shukla, P. K. and Mamun, A. A. 2002 *Introduction to Dusty Plasma Physics*. Bristol, UK: Institute of Physics.
- [6] Fortov, V. E. et al. 2005 *Phys. Rep.* **421**, 1.
- [7] Ishihara, O. 2007 *J. Phys. D* **40**, R121.
- [8] Shukla, P. K. and Eliasson, B. 2009 *Rev. Mod. Phys.* **81**, 25.
- [9] Morfill, G. E. and Ivlev, A. V. 2009 *Rev. Mod. Phys.* **81**, 1353.
- [10] Alfvén, H. 1942 *Nature* (London) **150**, 405.
- [11] D'Angelo, N. 1990 *Planet. Space Sci.* **38**, 1143.

- [12] Barkan, A., Merlino, R. L. and D'Angelo, N. 1995 *Phys. Plasmas* **2**, 3563.
- [13] Barkan, A., D'Angelo, N. and Merlino, R. 1995 *Planet. Space Sci.* **43**, 905.
- [14] Barkan, A., D'Angelo, N. and Merlino, R. 1996 *Planet. Space Sci.* **44**, 239.
- [15] Homann, A. et al. 1997 *Phys. Rev. E* **56**, 7138.
- [16] Merlino, R. L. et al. 1998 *Phys. Plasmas* **5**, 1590.
- [17] Winter, J. 1998 *Plasma Phys. Control. Fusion* **40**, 1201.
- [18] Thompson, C. et al. 1999 *IEEE Trans. Plasma Sci.* **27**, 146.
- [19] Nakamura, Y., Bailung, H. and Shukla, P. K. 1999 *Phys. Rev. Lett.* **83**, 1602.
- [20] Luo, Q. Z., D'Angelo, N. and Merlino, R. L. 1999 *Phys. Plasmas* **6**, 3455.
- [21] Hollenstein, C. 2000 *Plasma Phys. Control. Fusion* **42**, R93.
- [22] Nakamura, Y. and Sharma, A. 2001 *Phys. Plasmas* **8**, 3921 (2001).
- [23] Merlino, R. and Goree, J. 2004 *Phys. Today* **57**, 32.
- [24] Bandyopadhyay, P. et al. 2008 *Phys. Rev. Lett.* **101**, 065006.
- [25] Heinrich, J., Kim, S. H. and Merlino, R. 2009 *Phys. Rev. Lett.* **103**, 115002.
- [26] Bliokh, V. P. and Yaroshenko, V. V. 1985 *Sov. Astron.* **29**, 330.
- [27] de Angelis, U. et al. 1988 *J. Plasma Phys.* **40**, 399.
- [28] Rao, N. N., Shukla, P. K. and Yu, M. Y. 1990 *Planet. Space Sci.* **38**, 543.
- [29] Shukla, P. K. and Stenflo, L. 1992 *Astrophys. Space Sci.* **190**, 23.
- [30] Shukla, P. K. and Silin, V. P. 1992 *Physica Scripta* **45**, 508.
- [31] Bharuthram, R. and Shukla, P. K. 1992 *Planet. Space Sci.* **40**, 465.
- [32] Bharuthram, R. and Shukla, P. K. 1992 *Planet. Space Sci.* **40**, 973.
- [33] Shukla, P. K. and Varma, R. K. 1993 *Phys. Fluids B* **5**, 236.
- [34] Shukla, P. K. et al. 1993 *J. Geophys. Res.* **96**, 21343.
- [35] Verheest, F. 1994 *Space Sci. Rev.* **68**, 109.
- [36] Rao, N. N. 1995 *J. Plasma Phys.* **53**, 317.
- [37] Shukla, P. K. and Rahman, H. U. 1996 *Phys. Plasmas* **3**, 430.
- [38] Mamun, A. A., Cairns, R. A. and Shukla, P. K. 1996 *Phys. Plasmas* **3**, 702.
- [39] Mamun, A. A., Cairns, R. A. and P. K. Shukla 1996 *Phys. Plasmas* **3**, 2610.
- [40] Salimullah, M. 1996 *Phys. Lett. A* **215**, 296.
- [41] Melandsø, F. 1996 *Phys. Plasmas* **3**, 3890.
- [42] Mamun, A. A. 1998 *Phys. Scripta* **57**, 258.
- [43] Mamun, A. A. 1999 *Astrophys. Space Sci.* **268**, 443.
- [44] B. Farokhi et al. 1999 *Phys. Lett. A* **264**, 318.
- [45] Shukla, P. K. 1999 *Phys. Lett. A* **252**, 340.
- [46] Shukla, P. K. 2000 *Phys. Plasmas* **7**, 1044.
- [47] Shukla, P. K. 2001 *Phys. Plasmas* **8**, 1791.
- [48] Shukla, P. K. and Mamun, A. A. 2001 *Phys. Scripta* **64**, 351.
- [49] Shukla, P. K. and Mamun, A. A. 2001 *IEEE Trans. Plasma Sci.* **29**, 221.
- [50] Mamun, A. A. and Shukla, P. K. 2001 *Phys. Lett. A* **290**, 173.
- [51] Mamun, A. A., Shukla, P. K. and Bingham, R. 2001 *Phys. Lett. A* **298**, 179.
- [52] Ivlev, A. V. and Morfill, G. E. 2001 *Phys. Rev. E* **63**, 026412.
- [53] Popel, S. I. et al. 2001 *JETP Lett.* **74**, 396.
- [54] Shukla, P. K. 2002 *Phys. Lett. A* **306**, 135.
- [55] Mamun, A. A. and Shukla, P. K. 2002 *Phys. Plasmas* **9**, 1468.
- [56] Mamun, A. A. and Shukla, P. K. 2002 *Phys. Scripta T* **98**, 107.
- [57] Mamun, A. A. and Shukla, P. K. 2002 *IEEE Trans. Plasma Sci.* **30**, 720.
- [58] Mamun, A. A. and Shukla, P. K. 2003 *Phys. Plasmas* **11**, 1341.
- [59] Shukla, P. K. et al. 2003 *Phys. Rev. Lett.* **91**, 075005.

-
- [60] Shukla, P. K. and Eliasson, B. 2003 *JETP Lett.* **77**, 647.
- [61] Shukla, P. K. and Mamun, A. A. 2003 *New J. Phys.* **5**, 17.
- [62] Shukla, P. K. and Eliasson, B. 2004 *Phys. Plasmas* **11**, 584.
- [63] Eliasson, B. and Shukla, P. K. 2004 *Phys. Rev. E* **69**, 067401.
- [64] Mamun, A. A., Eliason, B. and Shukla, P. K. 2004 *Phys. Lett. A* **332**, 412.
- [65] Mamun, A. A. and Shukla, P. K. 2004 *Phys. Plasmas* **11**.
- [66] Mamun, A. A. et al. 2004 *Phys. Rev. Lett.* **92**, 095005.
- [67] Mamun, A. A. and Shukla, P. K. 2005 *J. Plasma Phys.* **71**, 143.
- [68] Mamun, A. A. 2008 *Phys. Lett. A* **372**, 1490.
- [69] Mamun, A. A. 2008 *Phys. Phys. Rev. E* **77**, 026406.
- [70] Verheest, F. and Pillay, S. R. 2008 *Phys. Plasmas* **15**, 013703.
- [71] Mamun, A. A. and Cairns, R. A. 2009 *Phys. Rev. E* **79**, 055401 (R).
- [72] Mamun, A. A. and Shukla, P. K. 2009 *Phys. Lett. A* **373**, 3161.
- [73] Mamun, A. A. and Shukla, P. K. 2009 *Europhys. Lett.* **87**, 25001.
- [74] Mamun, A. A. and Shukla, P. K. 2009 *Phys. Rev. E* **80**, 037401.
- [75] Mamun, A. A., Shukla, P. K. and Eliasson, B. 2009 *Phys. Rev. E* **80**, 046406.
- [76] Mamun, A. A. and Shukla, P. K. 2009 *Phys. Lett. A* **374**, 472.
- [77] Mamun, A. A. et al. 2009 *Phys. Plasmas* **16**, 114501.
- [78] Mamun, A. A. et al. 2010 *J. Plasma Phys.* **76**, 409.
- [79] Ikezi, H. 1986 *Phys. Fluids* **29**, 1764.
- [80] Thomas, H. et al. 1994 *Phys. Rev. Lett.* **73**, 652.
- [81] Chu, J. H. and Lin, I. 1994 *Phys. Rev. Lett.* **72**, 4009.
- [82] Hayashi, Y. and Tachibana, K. 1994 *Jpn. J. Appl. Phys.* **33**, L804.
- [83] Goree, J. 1999 *Phys. Rev. E* **59**, 7055.
- [84] Samsonov, D. et al. 1999 *Phys. Rev. Lett.* **83**, 3649.
- [85] Havnes, O. et al. 1996 *J. Vac. Sci. Technol. A* **14**, 525.
- [86] Thomas, H. et al. 2001 *Phys. Scripta T* **89**, 16.
- [87] Washimi, H. and Taniuti, T. 1966 *Phys. Rev. Lett.* **17**, 996.
- [88] Bernstein, I. B. et al. 1957 *Phys. Rev.* **108**, 546.
- [89] Sagdeev, R. Z. 1966 In: *Reviews of Plasma Physics*, Vol. 4 (ed. M. A. Leontovich). New York: Consultants Bureau, p. 23; Sagdeev, R. Z. 1979 *Rev. Mod. Phys.* **51**, 11.
- [90] Karpman, V. I. 1975 *Nonlinear Waves in Dispersive Media*, Oxford, UK: Pergamon, pp. 101–105.
- [91] Kaw, P. K. and Sen, A. 1998 *Phys. Plasmas* **5**, 3552.
- [92] Ichimaru, S., Iyetomi, H. and Tanaka, S. 1987 *Phys. Rep.* **149**, 91.
- [93] Slattery, W. L. et al. 1980 *Phys. Rev. A* **21**, 2087.
- [94] Berkovsky, M. A. 1992 *Phys. Lett. A* **166**, 365.